Complex-basis-function treatment of photoionization in the random-phase approximation

S. Yabushita and C. W. McCurdy
Department of Chemistry, The Ohio State University, Columbus, Ohio 43210

T. N. Rescigno
Lawrence Livermore National Laboratory, Livermore, California 94550

(Received 6 April 1987)

Complex-basis-function techniques are used to implement the equations of the random-phase approximation (RPA) in matrix form. This approach allows the direct extraction of total photoionization cross sections from a finite series of (complex) transition energies and oscillator strengths. The RPA is an effective means for including electron correlation effects on the photoionization of closed-shell atoms and molecules. The procedure demonstrated here provides a rigorous way of solving the RPA equations for continuum photoabsorption without resorting to numerical integration. The results of calculations on He and N_2 are presented. Correlation effects are found to significantly influence the threshold behavior of the N_2 photoionization cross sections.

I. INTRODUCTION

The development of reliable theoretical methods for calculating molecular photoionization cross sections is one of the most active fields in molecular physics. In contrast to atomic photoionization, the difficulty due to the nonspherical potentials in molecules has delayed the explicit calculations of final-state continuum wave functions even in the simple static-exchange approximation. This difficulty has led to the development of various L^2 methods.[1] One of the advantages of such methods is that many-body effects can readily be taken into account to any degree by adapting many existing techniques developed in bound-state theory.

We have previously shown that the complex-basis-function method provides a unified approach to the calculation of atomic and molecular photoionization cross sections with resonances incorporated naturally.[2] These methods can be employed at various levels of approximation from simple static-exchange[3] to large-scale configuration-interaction (CI) calculations,[4] and in some applications the working equations can be shown to arise from a variational principle for the frequency-dependent polarizability, the imaginary part of which yields the cross section.[2] Although most applications of these ideas have yielded total cross sections, we have recently shown that both partial cross sections and angular distributions can also be calculated with these techniques.[5]

An extension of this approach to the random-phase approximation (RPA) level is presented here. The RPA has been shown to provide a simple, effective way to study correlation effects in atoms and molecules; its strengths and limitations have been well documented.[6] The RPA has also been shown to be of great utility in atomic photoionization calculations, first by Altick and Glassgold[7] and later by Amus'ya and co-workers.[8] In these atomic applications the continuum RPA equations were solved by numerical integration, an approach not easily extended to molecular systems. More recently, Stieltjes imaging techniques,[9] together with approximate channel decoupling procedures, have been employed by Williams and Langhoff in RPA photoionization calculations using finite basis sets on H_2O (Ref. 10) and N_2.[11] Interesting applications of the RPA to atomic and molecular photoionizations were also performed by Zangwill *et al.*[12] in the local-density approximation.

The computational advantages of the RPA arise from the fact that only two-electron integrals involving two occupied (hole) orbitals and two unoccupied (particle) orbitals are involved. Therefore the integrals required are the same type [(*pphh*) and (*phph*)] as those in the static-exchange approximation, and the calculations presented here require little more computational effort than such calculations.

II. THEORY

The total photoabsorption cross section, $\sigma(\omega)$, can be written in terms of the imaginary part of the negative frequency component of the frequency-dependent polarizability, $\alpha(\omega)$,

$$\alpha(\omega)=-\lim_{\epsilon\to 0}\left\langle \Psi_0\mu \left| \frac{1}{E_0+\omega-H+i\epsilon} \right| \mu\Psi_0 \right\rangle , \tag{1}$$

$$\sigma(\omega)=\frac{4\pi\omega}{c}\mathrm{Im}\alpha(\omega) , \tag{2}$$

where Ψ_0 is the initial-state wave function with energy E_0, μ is the component of the dipole operator parallel to the polarization vector of the applied field, and c is the speed of light. Atomic units are used throughout this discussion.

The energy spectrum of the Hamiltonian, H, of course contains one or more continua. If H is approximated in a finite basis, the matrix eigenfunctions Φ_n and eigenvalues E_n provide an approximate spectral representation of Eq. (1) of the form

$$\alpha(\omega)\simeq-\sum_n \frac{d_{0n}d_{n0}}{E_0+\omega-E_n} , \tag{3}$$

where d_{n0} is a dipole transition moment $\langle\Phi_n\,|\,\mu\,|\,\Psi_0\rangle$. The eigenstates Φ_n and eigenvalues E_n satisfy

$$\langle\Phi_n\,|\,H\,|\,\Phi_m\rangle=\delta_{n,m}E_n . \tag{4}$$

If the usual Hermitian matrix representation is used, the eigenvalues will be real valued, as will the product of transition moments. Thus $\alpha(\omega)$ in Eq. (3) has no imaginary part in such a finite-basis approximation and it yields no information directly about the photoabsorption cross section.

On the other hand, the method of complex basis functions produces complex eigenvalues in the discretized continuum as well as complex dipole transition moments. We have previously shown that this procedure provides a rigorously convergent approximation to $\alpha(\omega)$ for real ω.[2]

The random-phase approximation is a simple approach to the study of correlation effects in the electronic spectra of atoms and molecules. It is most easily derived from the point of view of the equations of motion method[13] in which one solves for the operator $A^+(E)$ which generates an excited state of the Hamiltonian with excitation energy $\Delta E\equiv E-E_0$ when it operates on the ground state,

$$A^+(E)\,|\,0\rangle=|\,E\rangle , \tag{5}$$

and satisfies the equation

$$[H,A^+(E)]\,|\,0\rangle=\Delta E\,|\,E\rangle . \tag{6}$$

In the RPA, the operator $A^+(E)$ is restricted to have the form of a sum of single particle-hole excitations and deexcitations,

$$A^+(E)=\sum_{m,\alpha}(g_{m\alpha}c_m^\dagger c_\alpha-h_{m\alpha}c_\alpha^\dagger c_m) , \tag{7}$$

where $c^\dagger$ and c are second-quantized creation and annihilation operators and the indices α and m refer to Hartree-Fock hole and particle states, respectively, including the spin functions.

The working equations of the RPA are derived from Eqs. (5)–(7) by a linearization procedure which has been extensively discussed in the literature. The result is an equation for the amplitudes, $g_{m\alpha}$ and $h_{m\alpha}$, and the transition frequencies ΔE

$$\begin{bmatrix} \underline{A} & \underline{B} \\ -\underline{B} & -\underline{A} \end{bmatrix}\begin{bmatrix} \mathbf{g} \\ \mathbf{h} \end{bmatrix}=\Delta E\begin{bmatrix} \mathbf{g} \\ \mathbf{h} \end{bmatrix} , \tag{8}$$

where, for the singlet coupling case which follows throughout this study, the matrices $\underline{A}$ and $\underline{B}$ are given by

$$\begin{aligned} A_{m\alpha n\beta}&=(\varepsilon_m-\varepsilon_\alpha)\delta_{mn}\delta_{\alpha\beta}+2V_{\alpha nm\beta}-V_{\alpha n\beta m} , \\ B_{m\alpha n\beta}&=2V_{\alpha\beta mn}-V_{\alpha\beta nm} . \end{aligned} \tag{9}$$

From now on, the orbital indices refer to only the spatial part. In the above equations, ε_m and ε_α denote the closed-shell Hartree-Fock orbital energies of the particle and hole states, respectively, and the two-electron integrals are given by

$$V_{ijkl}=\int\int\phi_i^*(r_1)\phi_j^*(r_2)\frac{1}{r_{12}}\phi_k(r_1)\times\phi_l(r_2)d^3r_1d^3r_2 . \tag{10}$$

The dipole transition moment for a transition from the ground state to state $|\,E\rangle$ is given by

$$d_{0E}=\sqrt{2}\sum_{m,\alpha}[g_{m\alpha}(E)\langle\alpha\,|\,\mu\,|\,m\rangle+h_{m\alpha}(E)\langle m\,|\,\mu\,|\,\alpha\rangle] . \tag{11}$$

As mentioned above, the complex-basis-function implementation of the RPA equations which yields complex values of ΔE for continuum transitions is obtained by providing a complex basis of particle states. In addition, it is necessary to redefine the inner product without complex conjugation of the radial variables. This is the same prescription used in all previous complex-basis-function and complex-coordinate calculations and has been discussed in several review articles.[14] In the calculations presented here which ultimately make use of Cartesian Gaussian basis functions, the inner product is, in fact, defined with no complex conjugation at all.

The hole and particle orbitals are both eigenfunctions of the closed-shell Fock operator

$$F\phi_i=\varepsilon_i\phi_i , \tag{12}$$

with

$$F=-\tfrac{1}{2}\nabla^2+V_{\text{nuc}}+\sum_\alpha(2\hat{J}_\alpha-\hat{K}_\alpha) , \tag{13}$$

where V_{nuc} is the nuclear attraction potential and $\hat{J}_\alpha$ and $\hat{K}_\alpha$ are the usual Coulomb and exchange operators. There is no need in general to use complex basis functions to describe the hole states. Thus the complex basis of particle states can be obtained by diagonalizing F in a basis consisting of both real and complex Gaussians as described in Sec. IV.

III. IONIZATION THRESHOLDS IN THE RPA EQUATIONS

A note on the structure of the bound and continuous spectra of the RPA equations is in order at this point. The matrix RPA equations written in Eq. (8) are simply the matrix form of the following coupled integro-differential equations for the amplitudes $g_\alpha(r)$ and $h_\alpha(r)$,

$$(F-\varepsilon_\alpha-\Delta E)g_\alpha(r)+v_g\phi_\alpha(r)=0 , \tag{14a}$$

$$(F-\varepsilon_\alpha+\Delta E)h_\alpha(r)+v_h\phi_\alpha(r)=0 , \tag{14b}$$

where the coupling operators (for singlet spin coupling) are given by

$$\nu_g\phi_\alpha(1)=\sum_\beta\left[\int d^3r_2 h_\beta(r_2)\frac{1}{r_{12}}(2-P_{12})\phi_\beta(r_2)\phi_\alpha(r_1)+\int d^3r_2\phi_\beta(r_2)\frac{1}{r_{12}}(2-P_{12})g_\beta(r_2)\phi_\alpha(r_1)\right], \tag{15a}$$

$$\nu_h\phi_\alpha(1)=\sum_\beta\left[\int d^3r_2 g_\beta(r_2)\frac{1}{r_{12}}(2-P_{12})\phi_\beta(r_2)\phi_\alpha(r_1)+\int d^3r_2\phi_\beta(r_2)\frac{1}{r_{12}}(2-P_{12})h_\beta(r_2)\phi_\alpha(r_1)\right]. \tag{15b}$$

The amplitudes $h_\alpha(r)$ and $g_\alpha(r)$ are related to the $g_{m\alpha}$ and $h_{m\alpha}$ vectors of Eqs. (7) and (8) by

$$g_\alpha(r)=\sum_m g_{m\alpha}\phi_m(r)\ , \tag{16a}$$

$$h_\alpha(r)=\sum_m h_{m\alpha}\phi_m(r)\ . \tag{16b}$$

We wish to exhibit the limiting form of these equations as $r\to\infty$. The first sums in Eqs. (15a) and (15b) both approach zero exponentially in this limit since they are all proportional to bound occupied orbitals $\phi_\beta(r)$ or $\phi_\alpha(r)$. The remaining terms in Eqs. (15a) and (15b) all approach zero in the limit $r\to\infty$ at least as fast as $1/r$ with coupling between the various channel functions $g_\beta(r)$ and $h_\beta(r)$. Thus by dropping all terms in Eqs. (15a) and (15b) except those proportional to $g_\alpha(r)$ $[h_\alpha(r)]$, we obtain the limiting forms

$$(h^\alpha_{\rm IVO}-\varepsilon_\alpha-\Delta E)g_\alpha(r)\underset{r\to\infty}{\to}0\ , \tag{17a}$$

$$(h^\alpha_{\rm IVO}-\varepsilon_\alpha+\Delta E)h_\alpha(r)\underset{r\to\infty}{\to}0\ , \tag{17b}$$

where $h^\alpha_{\rm IVO}$ is the familiar improved virtual orbital (IVO) Hamiltonian which describes the interaction of an electron with the ionic target obtained by removing an electron from orbital ϕ_α,[15]

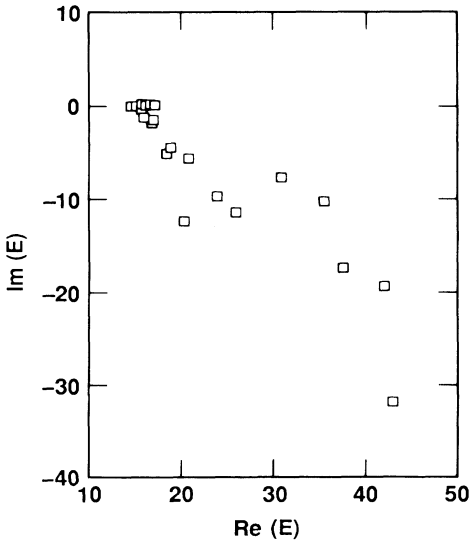

FIG. 1. Complex discretized spectrum for the case of N_2 in a two-channel ($3\sigma_g\to k\sigma_u$ and $1\pi_u\to k\pi_g$) RPA calculation. See text for computational details.

$$h^\alpha_{\rm IVO}=-\tfrac{1}{2}\nabla^2+V_{\rm nuc}+\sum_{\beta\neq\alpha}(2J_\beta-K_\beta)+J_\alpha+K_\alpha\ . \tag{18}$$

This Hamiltonian supports an infinite series of Rydberg states accumulating at zero energy, and thus the spectrum of Eq. (17a) for each α consists of bound states and a continuum beginning at $\Delta E=-\varepsilon_\alpha$. Therefore $g_\alpha(r)$ satisfies bound or continuum boundary conditions depending on whether ΔE is greater or less than $-\varepsilon_\alpha$. On the other hand, $h_\alpha(r)$ behaves like a closed-channel solution and decays exponentially because $\Delta E>0$ in all cases. Thus we see that the ionization thresholds in the RPA are in fact identical to the Koopmans theorem ionization potentials. Although the RPA does not improve the ionization potentials over those from Koopmans theorem, it does introduce coupling between the ionization continua. One effect of this coupling is that the Rydberg states converging to ionization thresholds corresponding to removal of electrons from inner-hole orbitals appear as autoionization states. On the other hand, the RPA does not include continua corresponding to the ionization of a target electron accompanied by excitation from a target-hole state to an unoccupied bound particle state. These continua are double excitations from the ground state.

The complex-basis-function implementation of the RPA equations moves the continua, which are discretized by the finite basis, into the lower half complex-energy plane. This important computational phenomena is illustrated in Fig. 1.

IV. RESULTS

A. Helium

We performed a test calculation on ionization of the He ground state in a $(10s13p)$ basis of uncontracted Gaussians. In this calculation the s-type Gaussians are all real valued, while the p-type Gaussians all have complex exponents and are thus of the form (p_x, for example)

$$\chi_i(\mathbf{r})=N(\zeta_i e^{-i\theta})x e^{-\zeta_i e^{-i\theta}r^2}\ , \tag{19}$$

where the normalization constant, $N(\zeta_i e^{-i\theta})$, is complex valued and is determined by requiring the integral of the square of the function, without complex conjugation, to be unity in accordance with the redefinition of the inner product in these calculations.

In Fig. 2 we show the results of this calculation using Eq. (3) for the frequency-dependent polarizability with transition energies and dipole transition moments computed with the RPA equations, Eqs. (8) and (11). The

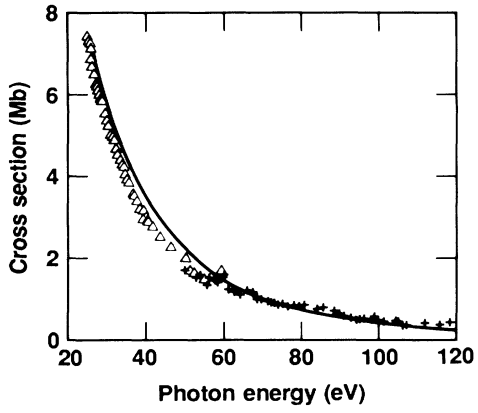

FIG. 2. Photoionization cross section of ground-state He. Solid curve, complex RPA results (length and velocity forms are graphically indistinguishable); triangles, measurement of Samson; crosses, measurements of Lowry *et al.*

close agreement between the cross sections obtained using the length and velocity forms of the dipole operator attests to the completeness of the complex and real parts of the basis set. These would agree identically in an exact numerical solution of the RPA equations.[16] Close agreement is also found between our calculations and previous numerical RPA calculations[17] (not shown in the figure) as well as with the experimental results.[18] The resonance structure near 60 eV which is evident in the experimental results is not present in the calculated cross section. This comes about from doubly excited states of the type $(2s2p)^1P$ which are not included in the RPA.

B. N_2

The Hartree-Fock equations for N_2 were solved in a real basis of $(9s5p1d)/[4s3p1d]$ Gaussians.[19] Several augmentations of this basis with real and complex Gaussians were tested in determining the particle states for these calculations. The complex functions in each case have exponents of the same form as those in Eq. (19), namely, $\zeta_j e^{-i\theta}$ with the same value of θ being used in all complex functions. For the results presented here, the augmented basis was chosen as follows.

In σ_g symmetry, real s-type functions with exponent 0.45 were centered on the nuclei along with complex functions whose exponents had moduli of 0.15 and 0.05. At the midpoint of the molecule, we used four additional complex s-type functions with $\xi_n = 0.0179/2.8^n$, $n = 1, \ldots, 4$, and eight additional d-type functions with $\xi_n = 0.26, \ldots, 0.076/2.1^n$, $n = 1, \ldots, 7$. The value of θ used in these calculations was 25°.

Previous separated-channel IVO (static-exchange) calculations of cross sections for ionization from the $3\sigma_g$ and $1\pi_u$ orbitals of N_2 were dominated by $\pi \rightarrow \pi^*$ and $\sigma \rightarrow \sigma^*$ resonance structures.[20] In the case of the $1\pi_u \rightarrow k\pi_g$ process, the IVO model produces a spurious π^* resonance feature at a photon energy of approximately 19 eV,[21] which should properly be a bound state of N_2 $(b'\,^1\Sigma_u^+)$ with a vertical energy of 14.4 eV. This cross section is shown in Fig. 3 together with the static-exchange cross section for the $3\sigma_g \rightarrow k\sigma_u$ channel. Coupling these two channels in the RPA moves the π^* resonance into the bound part of the spectrum. The resulting total cross section for ionization of the $3\sigma_g$ and $1\pi_u$ orbitals (in $^1\Sigma_u^+$ overall symmetry) is shown in Fig. 4.

Adding the $2\sigma_g \rightarrow k\sigma_u$ and $2\sigma_u \rightarrow k\sigma_g$ channels to this calculation, as shown in Fig. 5, brings the length and velocity forms of the cross section into better agreement, but does not qualitatively change the dominant features of the total cross section for $X\,^1\Sigma_g^+ \rightarrow k\,^1\Sigma_u^+$ ionization. Apart from a slight broadening, the $3\sigma_g \rightarrow k\sigma_u$ shape resonance is fundamentally unchanged from the two-channel result. The RPA cross section shows a significant threshold feature which must be associated with ionization of the $1\pi_u$ orbital because this is the lowest-energy channel in the RPA ionization spectrum. The Koopmans theorem ionization energies are 16.79 eV $(1\pi_u)$, 17.27 eV $(3\sigma_g)$, 21.26 eV $(2\sigma_u)$, and 40.28 eV $(2\sigma_g)$. Thus below 17.27 eV the total cross section is unambiguously associated with production of the $A\,^2\Pi_u$ state of N_2^+. It should be noted that the $3\sigma_g$ ionization energy leading to the $X^2\Sigma_g^+$ state of N_2^+ is physically the lowest threshold, and as is well known the Koopmans theorem ordering of the first two thresholds is reversed.

Evidently, a strong perturbation of the $n\pi_g$ Rydberg series by the $b'\,^1\Sigma_u^+$ state of N_2 is responsible for the threshold feature in the $A\,^2\Pi_u$ channel which is seen at the RPA level. Calculations employing several choices of the basis set parameters show that the threshold value itself is uncertain in our calculations by about 30%, but the sharp decline from threshold is apparently not a computational artifact. The width of this threshold feature, which is shown in the inset of Fig. 5, is evidently sensitive to channel coupling; the four-channel RPA calculations give a feature which is much narrower than the two-channel result shown in Fig. 4.

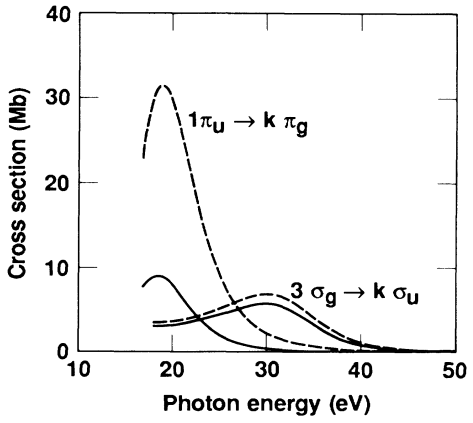

FIG. 3. Separated-channel IVO results for photoionization of N_2. Solid curve, velocity form; dashed curve, length form.

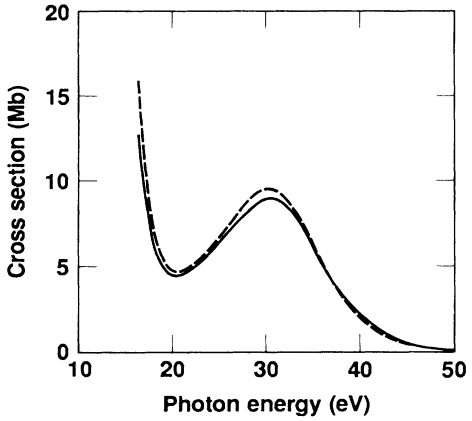

FIG. 4. Two-channel RPA photoionization cross section of N_2 in $^1\Sigma_u^+$ final-state symmetry.

This threshold feature is the only significant discrepancy between the calculations presented here and earlier RPA calculations of Williams and Langhoff using Stieltjes moment theory techniques.[11] We do not know whether the absence of this threshold feature in the Williams-Langhoff calculation is the result of inadequacies in the π_g basis they employed (lack of diffuse functions) or the approximate channel decoupling parameters used in their calculations. Experimental data for the partial photoionization cross section for production of the $A\ ^2\Pi_u$ state,[22] does show a general decline from threshold with autoionizing features[23] superimposed.

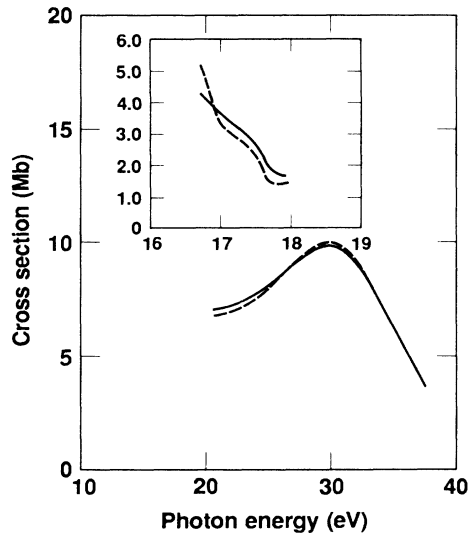

FIG. 5. Four-channel RPA photoionization cross section of N_2 in $^1\Sigma_u^+$ final-state symmetry. The inset shows the cross section in the threshold region. The interval between 18 and 20 eV (not shown) is dominated by autoionizing Rydberg states; converged results were not obtained in this region.

The theoretical results shown in Fig. 5 do not include contributions from $1\pi_u \rightarrow k\delta_g$ and $1\pi_u \rightarrow k\sigma_g$ transitions, which are not part of the $^1\Sigma_u^+$ final-state symmetry, but which do contribute to $A\ ^2\Pi_u$ production. We have not attempted to employ any channel decoupling approximations, such as those used by Williams and Langhoff, to separate the $1\pi_u$ ionization from $3\sigma_g$ ionization.

The photoabsorption spectrum of N_2 in the 17–19 eV region is dominated by Rydberg series converging to the $(2\sigma_u)^{-1}B\ ^2\Sigma_u^+$ state of N_2^+.[24] Inclusion of the $2\sigma_u \rightarrow k\sigma_g$ channel in the complex RPA calculations did produce several autoionizing states in this region, but the basis sets employed were evidently not rich enough to reliably resolve the resonance profiles against the background cross section. Moreover, the Koopmans value of 21.26 eV for the $2\sigma_u$ binding energy is almost 2.5 eV higher than the experimental ionization potential (IP) for the B state, which leads to errors of this magnitude in the positions of the autoionizing states. It would be possible to carry out RPA calculations by substituting experimental values of the IP's for the hole-state orbital energies, thereby forcing the Rydberg series to converge at the appropriate positions. One might also employ basis-set projection techniques of the type we previously used[4] to remove basis-set-dependent autoionizing states from the spectrum. We have not investigated these approaches in the present case.

V. CONCLUDING REMARKS

We have shown how complex-basis-function techniques can be used to solve the equations of the random-phase approximation in matrix form for continuum photoabsorption. The complex-basis-function implementation of the RPA provides an effective method for including electron correlation effects in the photoionization of closed-shell atoms and molecules, with computational effort comparable to that required in complex self-consistent-field (SCF) calculations.

We have illustrated the procedure with calculations of photoionization in He and N_2. Separated-channel IVO treatments of N_2 photoionization produce a spurious $\pi \rightarrow \pi^*$ resonance in the photoionization continuum. The principal result we have found is that channel coupling in the RPA moves this resonance into the bound region of the spectrum, but does leave a sharp threshold peak in the cross section associated with production of the $A\ ^2\Pi_u$ state of N_2^+. The broad σ^* shape resonance near 30 eV, however, does not appear to be sensitive to channel coupling effects.

ACKNOWLEDGMENTS

This work was performed under the auspices of the U.S. Department of Energy by the Lawrence Livermore National Laboratory under the terms of Contract No. W-7405-ENG-48. The work performed at the Ohio State University was supported by National Science Foundation Grant No. 8607496. One of us (C.W.M.) gratefully acknowledges support from the Camille and Henry Dreyfus Foundation.

[1]*Electron and Photon-Molecule Collisions,* edited by T. N. Rescigno, V. McKoy, and B. Schneider (Plenum, New York, 1979).
[2]T. N. Rescigno and C. W. McCurdy, Phys. Rev. A **31**, 624 (1985).
[3]C.-H. Yu, R. M. Pitzer, and C. W. McCurdy, Phys. Rev. A **32**, 2134 (1985).
[4]T. N. Rescigno, Phys. Rev. A **31**, 607 (1985).
[5]C. W. McCurdy and T. N. Rescigno, Phys. Rev. A **35**, 657 (1987).
[6]C. W. McCurdy, T. N. Rescigno, D. L. Yeager, and V. McKoy, in *Modern Theoretical Chemistry,* edited by H. F. Schaefer III (Plenum, New York, 1976), Vol. 2, p. 339.
[7]P. L. Altick and A. E. Glassgold, Phys. Rev. **133**, A632 (1964).
[8]M. Ya. Amus'ya, N. A. Cherepkov, and L. V. Chernysheva, Zh. Eksp. Teor. Fiz. **60**, 160 (1971) [Sov. Phys.—JETP **33**, 90 (1971)].
[9]P. W. Langhoff, in *Electron and Photon-Molecule Collisions,* edited by T. N. Rescigno, V. McKoy, and B. Schneider (Plenum, New York, 1979), p. 183.
[10]G. R. J. Williams and P. W. Langhoff, Chem. Phys. Lett. **60**, 201 (1979).
[11]G. R. J. Williams and P. W. Langhoff, Chem. Phys. Lett. **78**, 21 (1981).
[12]A. Zangwill and P. Soven, Phys. Rev. A **21**, 1561 (1980).
[13]D. J. Rowe, Rev. Mod. Phys. **40**, 153 (1968).
[14]W. P. Reinhardt, Annu. Rev. Phys. Chem. **33**, 223 (1982).
[15]W. J. Hunt and W. A. Goddard III, Chem. Phys. Lett. **3**, 414 (1969); **24**, 464 (1974).
[16]R. A. Harris, J. Chem. Phys. **50**, 3947 (1969).
[17]M. Ya. Amus'ya, N. A. Cherepkov, Dj. Zivanovic, and V. Radojevic, Phys. Rev. A **13**, 1466 (1976).
[18]J. A. R. Samson, Adv. At. Mol. Phys. **2**, 177 (1966); J. F. Lowry, D. H. Tomboulian, and D. L. Ederer, Phys. Rev. **137**, A1054 (1965).
[19]T. H. Dunning, J. Chem. Phys. **53**, 2823 (1970).
[20]T. N. Rescigno, C. F. Bender, B. V. McKoy, and P. W. Langhoff, J. Chem. Phys. **68**, 970 (1978).
[21]T. N. Rescigno and P. W. Langhoff, Chem. Phys. Lett. **51**, 65 (1977).
[22]E. W. Pummer, T. Gustafson, W. Gudat, and D. E. Eastman, Phys. Rev. A **15**, 2339 (1977).
[23]See, for example, D. C. Cartwright and T. H. Dunning, J. Phys. B **8**, L100 (1975), and references cited therein.
[24]M. Raoult, H. Le Rouzo, G. Raseev, and H. Lefebvre-Brion, J. Phys. B **16**, 4601 (1983).